# Relativistic configuration-interaction theory for atomic systems

Takashi Kagawa, Yoshie Honda, and Shuji Kiyokawa
*Department of Physics, Nara Women's University, Nara 630, Japan*
(Received 17 June 1991)

The relativistic configuration-interaction method with analytical relativistic Hartree-Fock-Roothaan (RHFR) basis functions for atomic systems is presented. One-electron functions used for constructing configuration state functions (CSF's) are obtained with the RHFR method in which the large and small components of the radial part of a four-component wave function are expanded in terms of an analytical basis set consisting of Slater-type orbitals. Numerical application of the method to neonlike atomic systems is carried out. It is shown that calculated excitation energies with the method are in good agreement with experiment. The $Z$-dependent behavior of the optical oscillator strengths for various electric-dipole transitions from the ground state in the systems is also given.

PACS number(s): 31.15.+q, 31.20.Di, 32.30.Rj, 32.70.Cs

## I. INTRODUCTION

Highly ionized atoms have attracted special interest in modern atomic physics and other related fields such as astrophysics and plasma physics [1]. Lines emitted from highly ionized atoms such as the first transition elements immersed in solar, stellar, and laboratory plasmas have been playing a very important role in modeling these matters. The development of experimental techniques such as the electron-beam ion sources or ion accelerators have made it possible to study the spectroscopic properties and scattering cross sections of various ion-collision processes with high accuracy [2]. In the analysis of the spectra observed in these experiments, accurate level structures and optical oscillator strengths for an atom in various charge states are required.

In the theoretical calculation of energy levels and oscillator strengths of highly ionized atoms, various relativistic effects as well as the correlation effects must be included in the theory adequately because the relativistic effects become large as the atomic number increases or as the degree of ionization in an atom becomes high. In the nonrelativistic quantum theory, the variational methods have widely been used for calculating energy levels in many-electron systems such as atoms and molecules. In this case the variational principle is used as a minimum principle as well as a stationary one. However, in relativistic quantum mechanics, the situation is very different from the nonrelativistic one. Brown and Ravenhall [3] have pointed out that the relativistic wave equation for many-body systems does not yield a normalizable wave function for a bound state because not only the positive-energy bound and continuum solutions but also negative-energy continuum ones are obtained with the wave equation. This means that there are an infinite number of configurations containing pairs of the positive- and negative-continuum states which yield the same energy as that for a bound state if the two-body interaction is neglected in the Hamiltonian. However, when this interaction is taken into account, these configurations are mixed with the normalizable bound state wave function in the configuration-interaction scheme, so that a total wave function becomes an unnormalizable function. Moreover, variational solutions for the relativistic wave equation cannot be obtained as an upper bound for the exact energy value of the ground state in a system since the spectrum of a relativistic Hamiltonian is not bounded from below due to the negative-energy continuum states.

Some people [3–5] proposed the no-pair approximation for the relativistic wave equation with the Dirac-Breit Hamiltonian for many-electron atomic systems to avoid the "continuum dissolution," that is, a mixing of positive- and negative-energy states obtained. The no-pair Hamiltonian contains a projection operator which can be expressed in terms of a set of positive-energy eigenfunctions for the single-electron Dirac wave equation. However, the positive-energy spectrum for the Dirac Hamiltonian with an appropriate one-electron potential in general consists of both discrete and continuum states so that one always encounters a difficulty of dealing with continuum wave functions in the calculation for energies in many-electron systems. Moreover, it seems that it is difficult to obtain a good energy with a relativistic calculation based on the no-pair approximation if the contribution from the continuum states to the total energy is not taken into account [6].

On the other hand, using the Dirac-Breit Hamiltonian for many-electron atoms, various relativistic atomic structure theories such as the Dirac-Hartree-Fock (DHF) one by use of the finite difference numerical method [7], analytical relativistic Hartree-Fock-Roothaan (RHFR) [8,9], multiconfiguration Dirac-Fock (MCDF) [10,11], analytical multiconfiguration relativistic Hartree-Fock-Roothaan (MCRHFR) [12] ones, relativistic many-body perturbation theory (RMBPT) [13–16], and relativistic $Z$-expansion theory [17] have so far been developed and successfully applied to atomic systems to obtain the relativistic effects on the energies and transition probabilities or optical oscillator strengths.

For the purpose of calculating energies for states consisting of a large number of multiplet terms in highly ionized atoms systematically, the relativistic configuration-

 

interaction method (RCI) is also one of the most powerful and efficient methods. Hagelstein [18] has made RCI calculations for highly ionized atoms, where a basis set for constructing the configuration state functions (CSF's) is obtained with the DHF calculation for corresponding fictitious closed-shell systems which have an electronic configuration containing excited orbitals with fractional occupation numbers. However, there have so far been reported few RCI calculations for atoms with large basis sets and the effectiveness of the method has not been investigated sufficiently. The whole scheme of the method is much simpler than that of the MCDF one, since the latter method requires one to solve extra coupled self-consistent field equations to determine one-electron wave functions in each calculation. Naturally accuracy of a RCI calculation deeply depends on one-electron functions used as a basis set.

Recently, the usefulness of the analytic basis set approach to accurate relativistic calculations for atoms such as the relativistic many-body perturbation ones [14–16] has been demonstrated. These calculations show that analytic basis set expansion methods can be used in approximating a projection operator introduced in the no-pair Hamiltonian in an efficient and easy-to-handle way. However, in this case the rigorous mathematical basis for the no-pair approximation is lost because each one-electron state obtained with the basis set expansion method is not necessarily an eigenstate for the Dirac wave equation containing an appropriate one-electron potential.

In this paper, we present the RCI method with a basis set in terms of analytical RHFR functions. By using Slater-type orbitals (STO's) with noninteger powers of $r$, a set of one-electron functions (OEF's) for constructing CSF's are obtained from the RHFR calculations [9] not only for the ground state but also some singly excited states in the systems under consideration. The RHFR calculations for excited states are carried out when OEF's belonging to the different symmetry from those contained in the ground-state configuration are needed in the RCI calculation.

In the RHFR calculation one sometimes encounters a difficulty that lower energies than the exact ground-state one for a system considered are obtained if one uses improper basis sets in the calculation because of the negative-continuum states in the energy spectrum of the Dirac-Breit Hamiltonian for atomic systems. In order to avoid the numerical failure, the relativistic virial theorem has been used to obtain a proper stationary RHFR solution, although it is not a necessary and sufficient condition for guaranteeing variational upper-bound solutions [8,9,19].

The operator $H_B(i,j)$ due to the Breit interaction between two electrons is neglected in the RHFR calculation but is treated by using the first-order perturbation theory in the RCI calculation. The radiative corrections or the Lamb-shift energies such as the self-energy and the vacuum polarization energy are not included in the present theory because they are higher-order corrections compared with the Coulomb or Breit interaction energies. The optical oscillator strengths for various transitions in a system are calculated relativistically with the RCI energies and the wave functions obtained.

Numerical application of the method to neonlike atomic systems is carried out. The calculated excitation energies and optical oscillator strengths are compared with experiment and those of the MCDF method [10,11], the RCI method of Hagelstein [18], and the Hartree-Fock with the relativistic correction (HFR) method [20].

## II. RELATIVISTIC CONFIGURATION-INTERACTION METHOD

For atomic systems, a relativistic Hamiltonian in atomic units is written as a sum of the Dirac Hamiltonian $H_D(i)$ and the two-electron operator $g(i,j)$ due to the Coulomb and the Breit interactions between electrons as follows:

$$H=\sum_i H_D(i)+\sum_{\substack{i\\ i<j}}\sum_j g(i,j)\ , \tag{1}$$

where

$$H_D(i)=c\boldsymbol{\alpha}_i\cdot\mathbf{p}_i+c^2\beta_i+V_N(r_i)\ , \tag{2}$$

$c$ is the velocity of light, and $\boldsymbol{\alpha}$ and $\beta$ are the Dirac operators in matrix form. $V_N(r)$ is the potential due to the nucleus which is assumed as a uniformly charged sphere, given by

$$V_N(r)=\begin{cases}-(Z/2R)(3-r^2/R^2) & \text{for } r\le R\\ -Z/r & \text{for } r>R\ ,\end{cases} \tag{3}$$

where $Z$ is the atomic number and $R$ is the radius of the nucleus which is in proportion to the cube of the atomic mass $A$ written as $R=2.3\times10^{-5}A^{-1/3}$ a.u.

The two-electron operator $g(i,j)$ is written as

$$g(i,j)=\frac{1}{r_{ij}}+H_B(i,j)\ , \tag{4}$$

where $H_B(i,j)$ is an operator for the Breit interaction given by

$$H_B(i,j)=-\frac{\boldsymbol{\alpha}_i\cdot\boldsymbol{\alpha}_j}{r_{ij}}-\tfrac{1}{2}(\boldsymbol{\alpha}_i\cdot\boldsymbol{\nabla}_i)(\boldsymbol{\alpha}_j\cdot\boldsymbol{\nabla}_j)r_{ij}\ . \tag{5}$$

In the present RCI calculation, the Breit interaction is treated using a first-order-perturbation theory.

We write a total configuration-interaction (CI) wave function $\Psi(\gamma JP)$ with a total angular momentum $J$ and parity $P$ as a linear combination of CSF's as

$$\Psi(\gamma JP)=\sum_n c_n\Phi_n(\gamma_n JP)\ , \tag{6}$$

where $\Phi(\gamma_n JP)$ is a CSF and $c_n$ is an expansion coefficient. $\gamma$ denotes a set of quantum numbers other than $J$ and $P$, which are needed to specify the state uniquely.

The RCI method deals with the secular equation for a Hamiltonian matrix with respect to CSF's. Each CSF is constructed as a product of OEF's obtained with the RHFR calculations described below.

### A. Calculation of RHFR one-electron basis functions

As details of the RHFR method for open-shell atoms have been described elsewhere [9], here we only give a brief description of the method in connection with the RCI scheme.

A four-component wave function $\psi(\mathbf{r})$ is expressed as

$$\psi_{n\kappa m}(\mathbf{r})=\frac{1}{r}\begin{bmatrix} P_{n\kappa}(r) & \chi_{\kappa m}(\theta,\phi) \\ iQ_{n\kappa}(r) & \chi_{-\kappa m}(\theta,\phi) \end{bmatrix} \tag{7}$$

where $P_{n\kappa}(r)$ and $Q_{n\kappa}(r)$ are the large and small components of the radial part of a wave function, respectively. $\chi_{\kappa m}(\theta,\phi)$ is a two-component spherical harmonic spinor and $\kappa$ is a relativistic angular momentum quantum number.

In the RHFR method, both $P_{n\kappa}(r)$ and $Q_{n\kappa}(r)$ are expanded in terms of the same STO's in the following form:

$$P_{n\kappa}(r)=\sum_i \xi_{n\kappa i} f_{\kappa i}(r) \tag{8a}$$

and

$$Q_{n\kappa}(r)=\sum_i \eta_{n\kappa i} f_{\kappa i}(r) , \tag{8b}$$

where $\xi$ and $\eta$ are expansion coefficients for the $P(r)$ and $Q(r)$, respectively. A STO $f_{\kappa i}(r)$ is written as

$$f_{\kappa i}(r)=(2\zeta_{\kappa i})^{\nu_{\kappa i}+1/2}[\Gamma(2\nu_{\kappa i}+1)]^{-1/2} r^{\nu_{\kappa i}} \exp(-\zeta_{\kappa i} r) , \tag{9}$$

where

$$\nu_{\kappa i}=n_i-1+[\kappa^2-(Z\alpha)^2]^{1/2} \quad \text{for } n_i=1,2,\ldots , \tag{10}$$

$\Gamma(2\nu_{\kappa i}+1)$ is a gamma function, and $\alpha$ the fine-structure constant.

The RHFR equation for open-shell atoms is the pseudoeigenvalue equations for closed- and open-shell vectors of the expansion coefficients and solved by iteration for the closed- and open-shell equations until self-consistency is obtained. The solutions for negative-energy states are not used since we are concerned with positive-energy states. All the real and virtual RHFR OEF's obtained can form a basis set for constructing CSF's in a RCI wave function. OEF's required in the RCI calculation are obtained from the RHFR calculations not only for the ground state but also for singly excited states. For example, in the case of neonlike atoms, the ground-state configuration is $1s^2 2s^2 2p_{1/2}^2 2p_{3/2}^4$ so that the RHFR calculation for the ground state yields OEF's belonging to the $s$, $p_{1/2}$, and $p_{3/2}$ symmetries. On the other hand, OEF's belonging to other $\kappa$ symmetry species such as $d_{3/2}$, $d_{5/2}$, $f_{5/2}$, etc. are obtained from the RHFR calculations for singly excited states having configurations of $1s^2 2s^2 2p_{1/2}^2 2p_{3/2}^3(n\kappa)$ for $n\kappa=3d_{3/2}$, $3d_{5/2}$, $4f_{5/2}$, etc.

In the RHFR calculation, optimization for the exponents in the STO's is important to obtain a good energy. However, a RHFR solution is not always obtained as an upper bound for the true ground-state energy in a system because of the negative-energy states appearing in the solutions for the relativistic wave equation. The relativistic virial theorem is used as a criterion for a stationary RHFR solution. The relativistic virial theorem is expressed as

$$\langle|T|\rangle=-\langle|V|\rangle , \quad E=\langle|M|\rangle , \tag{11}$$

where $\langle|T|\rangle$, $\langle|V|\rangle$, and $\langle|M|\rangle$ are the expectation values for the kinetic, potential, and rest-mass energy operators. In the RHFR calculation, the optimization of the orbital exponents in the STO's is carried out so as to obtain a lower energy among those which satisfy the relativistic virial theorem.

In addition to the problem of the unboundedness of the Hamiltonian described above, a problem of spurious solutions for the relativistic wave equation also lies in the RHFR calculation, where a spurious solution which corresponds to the lowest positive-energy state belonging to a positive $\kappa$ symmetry always appears. These unphysical solutions such as $1p_{1/2}$, $2d_{3/2}$, etc. are completely discarded in the RHFR calculation. However, a normal HF orbital belonging to a positive $\kappa$ symmetry is obtained as a function to be orthogonal to all the rest HF orbitals including the spurious one. This means that in order to obtain a good RHFR energy it is important to add some STO's to the basis set to describe an orbital for the spurious state adequately. Previously we have used STO's with the same principal quantum number as those of orbitals for spurious states for positive $\kappa$ symmetries such as $1p$, $2d$, etc. in the RHFR calculation, respectively, and obtained a good result for various atomic systems [9].

### B. Evaluation of Hamiltonian matrix elements

By using tensor algebra, various techniques in evaluating the matrix elements for one- and two-body operators have been developed [21–28]. The tensor recoupling transformation techniques in the second quantized form have also been used to evaluate Hamiltonian matrix elements in the MCRHFR theory by Kagawa [12]. Here we describe the method of calculating matrix elements for two-electron operators such as the Coulomb and the Breit interaction ones with respect to two CSF's in more detail. The method in the $j$-$j$ coupling scheme is almost the same as that in the $LS$ coupling case of Sasaki [28].

Let $a_{jm}^\dagger$ and $a_{jm}$ be creation and annihilation operators for a $jm$ state, respectively. They obey the anticommutation relations given by

$$\begin{aligned} &(a_{jm}, a_{j'm'}^\dagger)_+=\delta_{jj'}\delta_{mm'} , \\ &(a_{jm}^\dagger, a_{j'm'}^\dagger)_+=(a_{jm}, a_{j'm'})_+=0 . \end{aligned} \tag{12}$$

The $2j+1$ operators of $a_{jm}^\dagger$ for $-j\le m\le j$ form a complete set of a spherical tensor of rank $j$. This is not the case for $a_{jm}$. However, if one uses modified annihilation operators $\tilde{a}_{jm}$ given by

$$\tilde{a}_{jm}=(-1)^{j-m} a_{j,-m} , \tag{13}$$

$\{\tilde{a}_{jm}\}$ also form a complete set of a spherical tensor of rank $j$. The anticommutation relation for $\tilde{a}$ and $a^\dagger$ tensors is expressed as

$$[\tilde{a}_j \times a_{j'}^\dagger]^{JM} + (-1)^{j+j'-J}[a_{j'}^\dagger \times \tilde{a}_j]^{JM} = \sqrt{2j+1}\,\delta_{jj'}\delta_{J0}\delta_{M0} , \quad (14)$$

where $[\tilde{a}_j \times a_{j'}^\dagger]^{JM}$ means the tensor coupling leading to a resultant angular momentum $J$ and its component $M$.

A state arising from $N$ equivalent electrons in an $n\kappa$ relativistic atomic shell is specified by a total angular momentum quantum number $T$ and an ordering index $\lambda$ as a result of the angular momentum coupling for these equivalent electrons in the shell. We do not use the seniority scheme [24] here, since in this scheme one cannot uniquely specify a state containing more than two equivalent electrons in the $n\kappa$ shells with $j \geq \frac{9}{2}$. This restriction for the high-$j$ states can be removed if one uses an ordering index $\lambda$ for states with the same $J$ instead of $v$ to label them. We have developed a general computer program to calculate fractional parentage coefficients (FPC's) for $n\kappa$ shells with any number of equivalent electrons.

Using creation operators $a^\dagger$, a state $|\lambda T\rangle$ with $N$ electrons in the $n\kappa$ shell is written as

$$|\lambda T\rangle = [(a_{n\kappa}^\dagger)^N, \lambda T]|0\rangle , \quad (15)$$

where $|0\rangle$ denotes the vacuum state.

If an electronic configuration consists of two $n\kappa$ and $n'\kappa'$ shells with subtotal angular momentum quantum numbers $T$ and $T'$, respectively, a state with $J$ obtained with the coupling of the two angular momenta is given by

$$|\gamma J\rangle = [(\lambda T)\times(\lambda' T')]^J|0\rangle . \quad (16)$$

The quantum number $M$ of a component for $J$ is omitted because the total energy for a state with $J$ is not affected by any value of $M$.

By extending the coupling scheme to many-shell cases, a CSF with a total angular momentum quantum number $J$ is constructed by performing the step-by-step coupling of the angular momentum from the innermost core to the outermost $m$ valence shell in the following:

$$|\gamma J\rangle = [(a_m^\dagger)^{N_m}, \lambda_m T_m, [(a_{m-1}^\dagger)^{N_{m-1}}, \lambda_{m-1} T_{m-1}, [\cdots [(a_1^\dagger)^{N_1}, \lambda_1 T_1]^{J_1}]\cdots]^{J_{m-1}}]^J|0\rangle , \quad (17)$$

where $N_i$ is the number of electrons in the $i$th shell. $J_i$ is generated by the coupling of $J_{i-1}$ and $T_i$, $J_1 = T_1$ and $J_m = J$.

A two-electron operator $G$ in the second quantized form is written as [12]

$$G = \tfrac{1}{2}\sum_v \sum_{s,t,u,v} G_{stuv}^v \quad (18)$$

where

$$G_{stuv}^v = \langle st|g_v(1,2)|uv\rangle a_s^\dagger a_t^\dagger a_v a_u = (-1)^v(2v+1)^{-1/2}\langle s\|g^{(v)}(1)\|u\rangle\langle t\|g^{(v)}(2)\|v\rangle \times :([a_s^\dagger \times \tilde{a}_u]^v \times [a_t^\dagger \times \tilde{a}_v]^v)^0: , \quad (19)$$

and :: means the normal product for the creation and annihilation operators in $G_{stuv}^v$.

Now we describe the method of calculating the angular part of matrix elements for the Coulomb and the Breit interaction operators with respect to two CSF's. As the radial integrals for the operators are multiplicative factors for these matrix elements, we omit them in the following description.

The reduced matrix element for the Coulomb interaction operator with the wave functions in $j$-$j$ coupling is expressed by use of a Wigner's 3-$j$ symbol as

$$\langle \tfrac{1}{2} l_s j_s \| C^{(v)} \| \tfrac{1}{2} l_u j_u \rangle = (-1)^{j_s - 1/2}[(2j_s+1)(2j_u+1)]^{1/2} \times \begin{pmatrix} j_s & v & j_u \\ -\frac{1}{2} & 0 & \frac{1}{2} \end{pmatrix} \quad \text{for } l_s + v + l_u \text{ even} , \quad (20)$$

where $C^{(v)}$ is a spherical harmonic tensor and $l$ is an orbital angular momentum quantum number. The Breit interaction operator, which consists of the magnetic and the retardation terms, is written elsewhere [12,29]. It is expressed in terms of scalar products of the two tensors having the form

$$g_v(1,2) = \mathsf{T}^{(1L)v}(1)\cdot\mathsf{T}^{(1L')v}(2) , \quad (21)$$

where

$$\mathsf{T}^{(1L)v} = [\alpha^{(1)} \times C^{(L)}]^v , \quad (22)$$

and $\alpha^{(1)}$ is the Dirac operator of rank one. The reduced matrix element for $\mathsf{T}^{(1L)v}$ with respect to Dirac wave functions is written as a sum of those with respect to the large and small components between the wave functions. In this case the Pauli spin operator $\sigma^{(1)}$ instead of $\alpha^{(1)}$ in $\mathsf{T}^{(1L)v}$ appears in each reduced matrix element. The reduced matrix element is expressed with the Wigner 9-$j$ symbol as

$$\langle \tfrac{1}{2} l_s j_s \| [\sigma^{(1)} \times C^{(L)}]^v \| \tfrac{1}{2} l_u j_u \rangle = [(2j_s+1)(2v+1)(2j_u+1)]^{1/2} \begin{Bmatrix} \frac{1}{2} & l_s & j_s \\ \frac{1}{2} & l_u & j_u \\ 1 & L & v \end{Bmatrix} \langle \tfrac{1}{2}\|\sigma^{(1)}\|\tfrac{1}{2}\rangle\langle l_s\|C^{(L)}\|l_u\rangle , \quad (23)$$

where

$$\langle \tfrac{1}{2}\|\sigma^{(1)}\|\tfrac{1}{2}\rangle=\sqrt{3}\ , \tag{24}$$

and

$$\langle l_s\|C^{(L)}\|l_u\rangle=(-1)^{l_s}[(2l_s+1)(2l_u+1)]^{1/2}\begin{bmatrix} l_s & L & l_u \\ 0 & 0 & 0 \end{bmatrix} . \tag{25}$$

Let bra $\langle\gamma_n J|$ and ket $|\gamma_{n'}J\rangle$ states be two CSF's in Eq. (17) expressed in the second quantized form. The participating electrons labeled by $s$, $t$, $u$, and $v$ in the interaction can be selected so that the matrix element does not vanish. We usually have two combinations of two pairs of a creation and an annihilation operator in $G^{v}_{stuv}$ in Eq. (19), which correspond to the direct and exchange terms. In order to use the reduction formulas to evaluate the angular part of the matrix elements, the normal product of the operators specified by $s$, $t$, and $u$, and $v$ in Eq. (19) must be rearranged their positions by using the tensor recoupling transformation formulas. The arrangement for them is carried out in the same way as those for the creation operators in a CSF in Eq. (17), that is, in order from the innermost core to the outermost $m$ shell in the following form:

$$\langle\gamma_n J|([a_s^\dagger\times\tilde{a}_u]^v\times[a_t^\dagger\times\tilde{a}_v]^v)^{(0)}|\gamma_{n'}J\rangle = \sum_{\bar{J}} A_{\bar{J}}\langle\gamma_n J|\mathsf{Q}^{(0)}_{\bar{J}}|\gamma_{n'}J\rangle\ , \tag{26}$$

where

$$\mathsf{Q}^{(0)}_{\bar{J}}=[q_m,[q_{m-1},[\cdots[q_1]^{Q_1}]\cdots]^{Q_{m-1}}]^{(0)}\ , \tag{27}$$

and $q_s=a_s^\dagger$, $q_t=a_t^\dagger$, $q_u=\tilde{a}_u$, $q_v=\tilde{a}_v$. $q_i$ becomes the unit tensor if spectator electrons occupy the $i$th shell between two CSF's. $A_{\bar{J}}$ is a factor arising from the recoupling for the creation and annihilation operators in the arrangement and $\bar{J}$ is one of the resultant angular momentum quantum numbers due to the recoupling. When more than one participating electrons exist in the same shell, $q$ means a set of these operators.

The general reduction formula for the reduced matrix elements for tensor products of two tensors can directly be applied to the evaluation of the matrix elements for the second quantized operators in Eq. (26). Thus the reduced matrix element for the $\mathsf{Q}^{(0)}$ tensor in Eq. (26) can be expressed with the reduction formula [28] as

$$\langle\gamma_n J|\mathsf{Q}^{(0)}|\gamma_{n'}J\rangle=\langle[T_m\times J_{m-1}]^J|[q_m\times Q_{m-1}]^{(0)}|[T'_m\times J'_{m-1}]^J\rangle$$
$$=(-1)^{n(T'_m)\cdot n(Q_{m-1})}\langle T_m\|q_m\|T'_m\rangle\langle J_{m-1}\|Q_{m-1}\|J'_{m-1}\rangle(2J+1)\begin{bmatrix} T_m & J_{m-1} & J \\ T'_m & J'_{m-1} & J \\ q_m & Q_{m-1} & 0 \end{bmatrix} \tag{28}$$

where $n(T'_m)$ and $n(Q_{m-1})$ indicate the number of operators involved in $T'_m$ and $Q_{m-1}$. If $q_m$ consists of a single operator or complex ones appearing in the normal product in $G$ in Eq. (19), $\langle T_m\|q_m\|T'_m\rangle$ is evaluated in terms of a fractional parentage coefficient [23,24,27] for the $m$th shell. If $q_m$ is the unit tensor,

$$\langle T_m\|q_m\|T'_m\rangle=(2T_m+1)^{1/2}\delta_{T_m,T'_m}\ . \tag{29}$$

The same formula can be applied to the reduced matrix element $\langle J_{m-1}\|Q_{m-1}\|J'_{m-1}\rangle$ in the next step of the calculation. So $\langle J_i\|Q_i\|J'_i\rangle$ for the $i$th atomic shell is in general given by

$$\langle J_i\|Q_i\|J'_i\rangle=\prod_{k=1}^{i} L_k\ , \tag{30}$$

where

$$L_k=(-1)^{n(T'_k)\cdot n(Q_{k-1})}[(2J_k+1)(2Q_k+1)(2J'_k+1)]^{1/2} \times\begin{bmatrix} T_k & J_{k-1} & J_k \\ T'_k & J'_{k-1} & J'_k \\ q_k & Q_{k-1} & Q_k \end{bmatrix}\langle T_k\|q_k\|T'_k\rangle\ . \tag{31}$$

In evaluating the matrix element for the normal product of operators in $G$ in Eq. (19) with the formula, one is only required to prepare appropriate FPC's for the shells specified by $s$, $t$, $u$, and $v$. The merit of using the tensor recoupling transformation techniques in the second quantized form is that it is the straightforward iterative calculation without any procedure of antisymmetrization of wave functions and special treatment of the FPC's for atomic shells related to the matrix element.

### C. Relativistic transition probabilities and oscillator strengths

For highly ionized atoms, the relativistic effects on the energy levels and wave functions become large. This leads to significant changes in the transition energies and probabilities for the optical transitions in the systems from corresponding values of nonrelativistic calculations. So, it is very interesting to calculate transition probabilities or oscillator strengths for various optical transitions because the accuracy of calculated energies and wave functions obtained can be seen by comparing them with experiment.

The relativistic transition probability for an optical transition in an atomic system can be obtained by use of the time-dependent perturbation theory with the Born

approximation for the transition matrix ($T$ matrix) [30,31], where the $T$ matrix is given by the matrix element for the interaction Hamiltonian between atomic electrons and the radiation field with respect to the initial and final atomic states. The multipole expansion of the electromagnetic field leads to the total transition probability as a sum of those for all multipole electric- and magnetic-type transitions. The spontaneous emission probability for the transition from an upper $|b\rangle$ to a lower $|a\rangle$ state is written as

$$A_{b\to a}=2\alpha\omega\left|\sum_L[\langle b|M^L(e)|a\rangle+\langle b|M^L(m)|a\rangle]\right|^2, \tag{32}$$

where $\alpha$ is the fine-structure constant and $\omega$ is the transition frequency. $M^L(e)$ and $M^L(m)$ stand for the operators for the $2^L$ pole electric- and magnetic-type transitions, respectively. The expression of the matrix element for the transition operators $M^L$ in Eq. (29) with the RCI wave functions is given by

$$\langle b|M^L|a\rangle=\sum_n\sum_{n'}c_nc_{n'}\left[\sum_s\sum_t\left[-\frac{\langle j_s\|h^L\|j_t\rangle}{\sqrt{2L+1}}\langle\gamma_nJ_b\|[a_s^\dagger\times\tilde{a}_t]^L\|\gamma_{n'}J_a\rangle\right]\right] \tag{33}$$

where $c_n$ and $c_{n'}$ are the expansion coefficients for CSF's in the RCI wave functions for the upper $\langle b|$ and lower $|a\rangle$ states, respectively.

A single-electron operator $h^L(e)$ for the electric-type transition in Eq. (33) contains a gauge $G$. The matrix element for it is given by

$$\langle j_s\|h^L(e)\|j_t\rangle=\{G(\Upsilon_s+\Upsilon_l)+\Upsilon_t\}, \tag{34}$$

where $\Upsilon_s$, $\Upsilon_l$, and $\Upsilon_t$ are the transition matrix elements for the scalar, longitudinal, and transverse photons between the two states. The expression for them is complex and lengthy and given elsewhere [30,31]. The value of the transition probability is not free from the choice of $G$ when the exact wave functions for a system cannot be used, whereas $\Upsilon_s+\Upsilon_l=0$ if they are evaluated with the exact wave functions for the system. Since an exact wave function for a many-electron system is hard to obtain, one usually uses special values of $G=-[(L+1)/L]^{1/2}$ and $G=0$ in the evaluation of the matrix element for $h^L(e)$, which correspond to the length and velocity forms in the nonrelativistic limit, respectively.

In the evaluation of the matrix elements for $[a_s^\dagger\times\tilde{a}_t]^L$ involved in Eq. (34) with the RCI wave functions, one can also use the same reduction formula in Eq. (28) as that used for two-electron operators. Before doing this, one has to arrange the operator $[a_s^\dagger\times\tilde{a}_t]^L$ in the same order of atomic shells as that for CSF's in Eq. (17).

It is convenient to use the oscillator strengths instead of the transition probability if one compares the theoretical results with intensities of spectra observed. The relativistic oscillator strength for electric- and magnetic-type transitions in atomic units is written in terms of the relativistic transition probability $A_{b\to a}$ as

$$f_{a\to b}=\frac{2J_b+1}{2J_a+1}\frac{1}{2\alpha^3\omega^2}A_{b\to a}. \tag{35}$$

Finally the flowchart of the RCI calculation for energy levels and optical oscillator strengths in an atomic system is shown in Fig. 1.

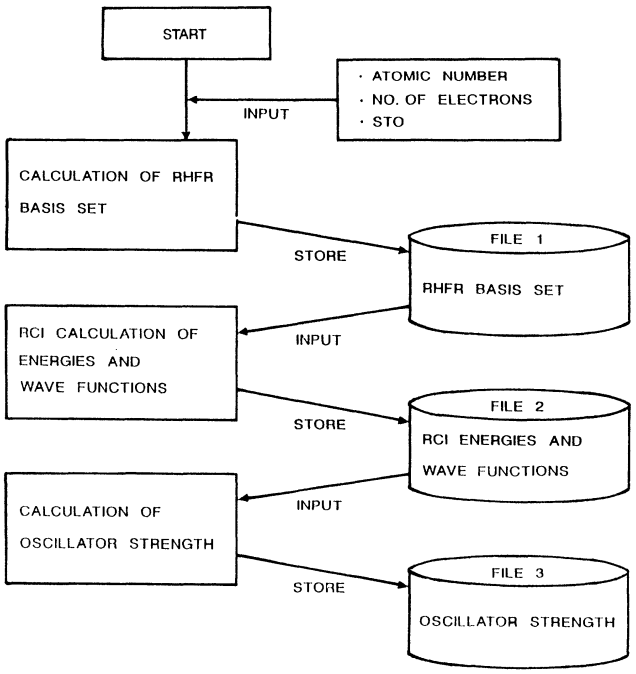


FIG. 1. Flowchart of the atomic structure calculation with the RCI method.

## III. CALCULATED RESULTS FOR NEONLIKE SYSTEMS

Now we apply the RCI method to neon isoelectronic sequence to see the effectiveness of the method. The neonlike systems picked here are $Ar^{8+}(Z=18)$, $Ti^{12+}(Z=22)$, $Fe^{16+}(Z=26)$, $Se^{24+}(Z=34)$, $Kr^{26+}(Z=36)$, $Mo^{32+}(Z=42)$, $Ag^{37+}(Z=47)$, $Xe^{44+}(Z=54)$, $Ba^{46+}(Z=56)$, $W^{64+}(Z=74)$, and $U^{82+}(Z=92)$.

First we carry out the RHFR calculations by use of STO's to obtain a set of OEF's for constructing the CSF's in Eq. (6). The number of STO's used for the systems considered is 8 for $s_{1/2}$, 8 for $p_{1/2}$, 6 for $p_{3/2}$, 6 for $d_{3/2}$, 6 for $d_{5/2}$, 6 for $f_{5/2}$, and 6 for $f_{7/2}$, where they consist of some sets of two STO's with the same $n_i$ but different orbital exponents of $\zeta_{\kappa i}$ and $\zeta'_{\kappa i}$, the so-called double-zeta

basis set. For $\kappa > 0$, STO's with the same principal quantum number $n_i$ as that of a spurious-state orbital such as $1p$ STO's etc. are included in the basis set to describe it adequately. An optimum RHFR energy can be obtained by varying orbital exponents in STO's so as to satisfy the relativistic virial theorem in Eq. (11).

In order to facilitate the optimization of the orbital exponents in the RHFR calculation, the values of exponents in the STO's belonging to $\kappa$ symmetry are taken as a function of a principal quantum number $n_i$ in $\nu_{\kappa i}$ in Eq. (10) and a variational parameter $\delta_\kappa$ for $\kappa$ symmetry, given by

$$\zeta_{\kappa i} = \delta_\kappa / (n_i)^p , \tag{36}$$

and

$$\zeta'_{\kappa i} = q \zeta_{\kappa i} , \tag{37}$$

where $p$ and $q$ are parameters appropriately chosen for each system and fixed during the RHFR calculation. So these constraints for the orbital exponents lead to only one parameter $\delta_\kappa$ needed to determine exponents in all STO's belonging to $\kappa$ symmetry. We choose $p = q = 1.5$ for all the systems considered here except for the $W^{64+}$ and $U^{82+}$ ions, $p = q = 2.0$ for $W^{64+}$ and $p = q = 2.5$ for $U^{82+}$. $\delta_\kappa$ is varied in the RHFR calculation to obtain an optimum RHFR energy.

As has been mentioned in Sec. II, OEF's for $s_{1/2}$, $p_{1/2}$, and $p_{3/2}$ symmetries are obtained from the RHFR calculation for the ground state and those belonging to $d_{3/2}$, $d_{5/2}$, $f_{5/2}$, and $f_{7/2}$ ones for excited states having the configuration of $1s^2 2s^2 2p_{1/2}^2 2p_{3/2}^3 (n\kappa)$ with the largest $J$ in the systems under consideration. It is noted that all the OEF's obtained form an orthonormal set. We assume that the positive-energy projection operator in the no-pair Hamiltonian for systems can effectively be approximated with the basis set.

TABLE I. Optimized parameter $\delta_\kappa$ for orbital exponents $\zeta_{i\kappa}$ and $\zeta'_{i\kappa}$ in double-zeta STO's obtained with the RHFR calculation for neonlike $Fe^{16+}$ and $Xe^{44+}$, where $\zeta_{i\kappa} = \delta_\kappa / n_i^{1.5}$ and $\zeta'_{i\kappa} = 1.5 \zeta_{i\kappa}$.

| Symmetry | Number of STO's | $n_i$ in STO's | $\delta_\kappa$ $Fe^{16+}$ | $\delta_\kappa$ $Xe^{44+}$ |
|---|---|---|---|---|
| $s_{1/2}$ | 8 | 1–4 | 25.232 52 | 45.151 12 |
| $p_{1/2}$ | 8 | 1–4 | 26.190 50 | 66.162 74 |
| $p_{3/2}$ | 6 | 2–4 | 26.190 51 | 57.322 43 |
| $d_{3/2}$ | 6 | 2–4 | 34.394 30 | 56.700 00 |
| $d_{5/2}$ | 6 | 3–5 | 26.000 00 | 55.096 20 |
| $f_{5/2}$ | 6 | 3–5 | 26.000 00 | 54.000 00 |
| $f_{7/2}$ | 6 | 4–6 | 25.946 12 | 54.000 00 |

Using 23 OEF's consisting from the $1s$ up to $5f_{7/2}$ RHFR functions, we carry out the RCI calculations to obtain the energies for even-parity states with $J = 0$–5 and odd-parity ones with $J = 0$–4 in $Fe^{16+}$ and $Xe^{44+}$ ions. The optimized values of the parameter $\delta_\kappa$ obtained with the RHFR calculation for these ions are listed in Table I. CSF's used in the RCI calculation are the ground configuration and all the possible single-excitation CSF's with the RHFR basis set used. In addition to the single-excitation CSF's, we use the $n = 2 \rightarrow 3$ double-excitation CSF's represented by the $(2p_{3/2})^2 \rightarrow (3\kappa)^2$ excitation from the ground state for even-parity states to take the electron correlation effects into account in the calculation adequately, where $3\kappa$ stands for $3s$, $3p_{1/2}$, $3p_{3/2}$, $3d_{3/2}$, and $3d_{5/2}$. In Figs. 2

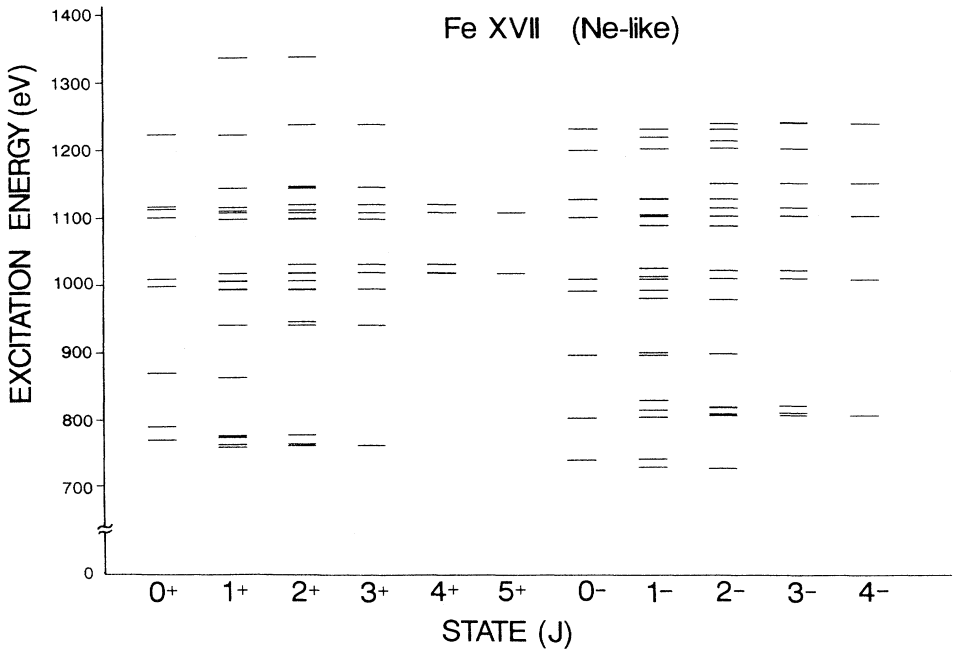


FIG. 2. Singly excited levels up to $n = 5$ for even-parity states with $J = 0$–5 and odd-parity ones with $J = 0$–4 in Fe XVII (neonlike). $J\pm$ denotes even- and odd-parity states with $J$, respectively.

and 3, calculated excitation energies from the ground-state energy for all the singly excited states with $n \leq 5$ in $Fe^{16+}$ and $Xe^{44+}$ are shown, respectively. It is seen from the figures that the relative spacing of the energy levels between the two systems changes because of the difference of the intermediate coupling in the wave function obtained through the RCI calculation between these systems.

In Table II, the RCI excitation energies from the ground state to singly excited ones with $n=3$ in $Fe^{16+}$ are compared with other theoretical results [32,33] and experiment [34]. Our RCI results are slightly large compared with two other theoretical values and experiment. This arises mainly for two reasons: One is that the Lamb shift or QED corrections are not taken into account in our RCI theory, since it is considered that the difference of the corrections between the $L$- and $M$-shell electrons is larger than that between the electrons in the same shell. The other is due to the basis set used: A set of OEF's obtained with the RHFR calculations is more preferable to obtain the energy for the ground state than those for excited states because the set commonly used in the RCI calculations has core orbitals obtained for the ground state in the systems. This leads to a little more energy

TABLE II. Comparison of the excitation energies from the ground state to excited states with $n=3$ in neonlike Fe($Z=26$) in $cm^{-1}$.

| State | RCI | RCI[a] | HFR[b] | Expt.[c] |
|---|---|---|---|---|
| $2s^22p^6$ ($^1S_0$) | 0 | 0 | 0 | 0 |
| $2s^22p^53s$ $(\frac{3}{2},\frac{1}{2})^o_2$ | 5 861 127 | 5 854 100 | 5 844 472 | 5 852 700 |
| $2s^22p^53s$ $(\frac{1}{2},\frac{1}{2})^o_1$ | 5 875 609 | 5 869 700 | 5 859 198 | 5 864 770 |
| $2s^22p^53s$ $(\frac{1}{2},\frac{1}{2})^o_0$ | 5 962 151 | 5 957 000 | 5 946 639 | |
| $2s^22p^53s$ $(\frac{1}{2},\frac{1}{2})^o_1$ | 5 969 957 | 5 966 800 | 5 956 000 | 5 960 870 |
| $2s^22p^53p$ $(\frac{3}{2},\frac{1}{2})^e_1$ | 6 109 418 | 6 097 800 | 6 094 955 | |
| $2s^22p^53p$ $(\frac{3}{2},\frac{1}{2})^e_2$ | 6 134 205 | 6 125 900 | 6 122 516 | |
| $2s^22p^53p$ $(\frac{3}{2},\frac{3}{2})^e_3$ | 6 138 237 | 6 138 800 | 6 134 946 | |
| $2s^22p^53p$ $(\frac{3}{2},\frac{3}{2})^e_1$ | 6 143 687 | 6 148 300 | 6 144 426 | |
| $2s^22p^53p$ $(\frac{3}{2},\frac{3}{2})^e_2$ | 6 153 238 | 6 162 500 | 6 158 046 | |
| $2s^22p^53p$ $(\frac{3}{2},\frac{3}{2})^e_0$ | 6 195 122 | 6 208 000 | 6 203 689 | |
| $2s^22p^53p$ $(\frac{1}{2},\frac{1}{2})^e_1$ | 6 228 788 | 6 224 600 | 6 221 146 | |
| $2s^22p^53p$ $(\frac{1}{2},\frac{3}{2})^e_1$ | 6 254 298 | 6 250 300 | 6 246 049 | |
| $2s^22p^53p$ $(\frac{1}{2},\frac{3}{2})^e_2$ | 6 258 885 | 6 253 500 | 6 248 856 | |
| $2s^22p^53p$ $(\frac{1}{2},\frac{1}{2})^e_0$ | 6 360 681 | 6 376 400 | 6 361 052 | |
| $2s^22p^53d$ $(\frac{3}{2},\frac{3}{2})^o_0$ | 6 472 881 | 6 468 500 | 6 462 777 | |
| $2s^22p^53d$ $(\frac{3}{2},\frac{3}{2})^o_1$ | 6 482 760 | 6 476 200 | 6 470 935 | 6 471 800 |
| $2s^22p^53d$ $(\frac{3}{2},\frac{5}{2})^o_4$ | 6 497 840 | 6 491 800 | 6 487 376 | |
| $2s^22p^53d$ $(\frac{3}{2},\frac{5}{2})^o_2$ | 6 497 939 | 6 490 900 | 6 486 043 | |
| $2s^22p^53d$ $(\frac{3}{2},\frac{3}{2})^o_3$ | 6 504 263 | 6 498 500 | 6 492 956 | |
| $2s^22p^53d$ $(\frac{3}{2},\frac{3}{2})^o_2$ | 6 516 582 | 6 512 279 | 6 506 860 | |
| $2s^22p^53d$ $(\frac{3}{2},\frac{5}{2})^o_3$ | 6 528 114 | 6 520 700 | 6 515 730 | |
| $2s^22p^53d$ $(\frac{3}{2},\frac{5}{2})^o_1$ | 6 564 236 | 6 559 900 | 6 553 145 | 6 552 200 |
| $2s^22p^53d$ $(\frac{1}{2},\frac{3}{2})^o_2$ | 6 602 564 | 6 600 900 | 6 594 981 | |
| $2s^22p^53d$ $(\frac{1}{2},\frac{5}{2})^o_2$ | 6 610 361 | 6 606 900 | 6 601 670 | |
| $2s^22p^53d$ $(\frac{1}{2},\frac{5}{2})^o_3$ | 6 614 948 | 6 611 600 | 6 606 055 | |
| $2s^22p^53d$ $(\frac{1}{2},\frac{3}{2})^o_1$ | 6 680 481 | 6 674 500 | 6 664 325 | 6 660 000 |
| $2s2p^63s$ $(\frac{1}{2},\frac{1}{2})^e_1$ | 6 955 442 | 6 950 300 | | |
| $2s2p^63s$ $(\frac{1}{2},\frac{1}{2})^e_0$ | 7 006 626 | 7 002 700 | | |
| $2s2p^63p$ $(\frac{1}{2},\frac{1}{2})^o_0$ | 7 220 122 | 7 214 100 | | |
| $2s2p^63p$ $(\frac{1}{2},\frac{1}{2})^o_1$ | 7 225 645 | 7 217 800 | | 7 198 900 |
| $2s2p^63p$ $(\frac{1}{2},\frac{3}{2})^o_2$ | 7 243 722 | 7 236 600 | | |
| $2s2p^63p$ $(\frac{1}{2},\frac{3}{2})^o_1$ | 7 260 860 | 7 251 600 | | 7 235 900 |
| $2s2p^63d$ $(\frac{1}{2},\frac{3}{2})^e_1$ | 7 579 365 | 7 578 100 | | |
| $2s2p^63d$ $(\frac{1}{2},\frac{3}{2})^e_2$ | 7 580 405 | 7 579 000 | | |
| $2s2p^63d$ $(\frac{1}{2},\frac{5}{2})^e_3$ | 7 582 893 | 7 581 000 | | |
| $2s2p^63d$ $(\frac{1}{2},\frac{5}{2})^e_2$ | 7 624 886 | 7 620 200 | | |

[a]Reference [32].
[b]Reference [33].
[c]Reference [34].

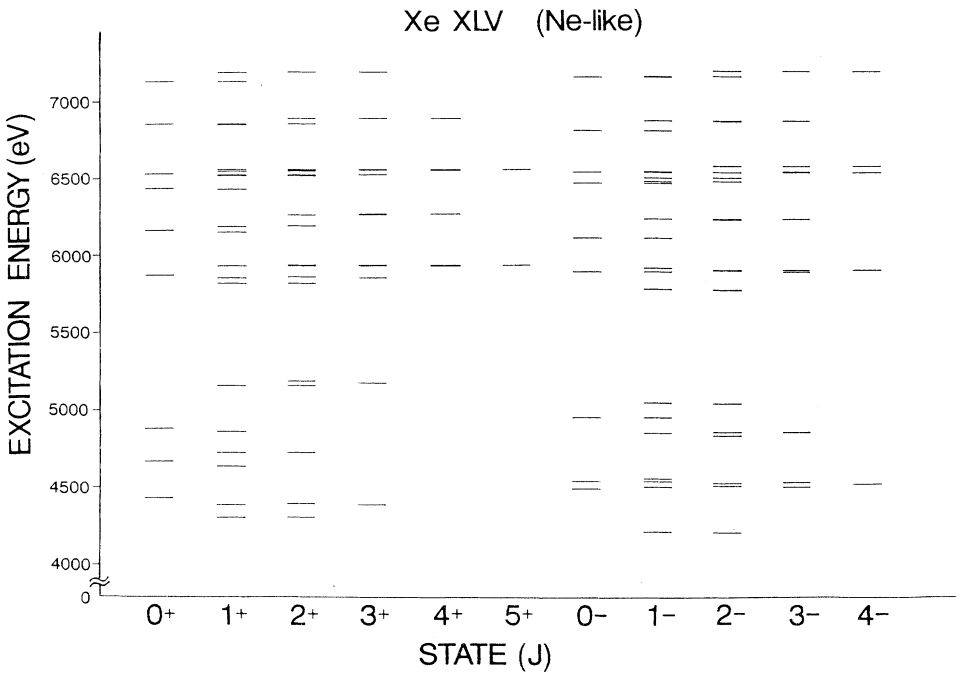


FIG. 3. Singly excited levels up to $n=5$ for even-parity states with $J=0-5$ and odd-parity ones with $J=0-4$ in Xe XLV (neonlike).

drop of the total RCI energy for the ground state than those for all excited states considered.

In fusion study, various specific elements such as the first transition elements or Mo become important because they are used to construct a fusion reactor. On the other hand, this conversely causes the radiation loss problem if they are sputtered from the wall of the reactor into fusion plasmas. For neonlike systems, many intense lines due to the electric-dipole ($E1$) transitions between the ground state ($J=0$) and excited states ($J=1$) have been observed and identified. There have been many comparison data for spectroscopic lines observed in highly ionized atomic system including these elements related especially to the astrophysics or fusion study.

In Tables III–VII, the RCI transition energies for the $E1$ transitions between the ground and the singly excited states in neonlike Ar, Ti, Fe, Ni, and Mo ions are compared with experiment, respectively. In these tables the calculated oscillator strengths are also listed together with those obtained with the relativistic random phase approximation (RRPA) method by Shorer [35] or those in the atomic transition tables of Wiese and his collaborators cited by other people in the compilation of the experimental data [34,36,37]. We consider in detail the accuracy of our RCI results for these systems in the tables.

### A. $Ar^{8+}$ ion

The RCI excitation energies for $Ar^{8+}$ are compared with the experimental ones [38] in Table III. In the intermediate coupling, it often happens that the main configuration for a state cannot necessarily be represented with a single CSF in either pure $LS$ or $j$-$j$ couplings. In the $Ar^{8+}$ case, the three CSF's generated by the $2p_{1/2}\rightarrow 3d_{3/2}$, $2p_{3/2}\rightarrow 3d_{3/2}$, and $2p_{3/2}\rightarrow 3d_{5/2}$ excitations from the ground configuration are so strongly mixed that it is difficult to pick the main configuration especially for the fourth lowest excited state in the table. We write the $1s^2 2s^2 2p^5 3d\ (\frac{1}{2},\frac{3}{2})_1^o$ as the main configuration for both the fourth and fifth lowest excited states in the table because of the largest expansion coefficient for the CSF. This means that the wave function for $Ar^{8+}$ can still be described well with $LS$ coupling rather than the $j$-$j$ one. This fact has already been shown by Shorer by transforming the RRPA wave functions in $j$-$j$ coupling into the $LS$ coupling ones, where each state can be well described with a main configuration in $LS$ coupling. This means that the spin-orbit term is not so large compared with the Coulomb interaction energies in this ion.

It is seen from the table that errors for most RCI results except those for states arising from the excitation of $2s$ or $2p_{1/2}$ electrons are within about 0.5%. Large error in the calculated transition frequencies for some singly excited states due to the transition of the inner $2s$ or $2p_{1/2}$ electrons will be seen in the tables for other ions such as $Ti^{12+}$, $Fe^{16+}$, and $Ni^{18+}$ systems. It mainly arises from the lack of the Lamb shift or the QED corrections in our RCI theory.

The RCI oscillator strengths for the $n=2\rightarrow 3$ transition lines are compared in the table with the RRPA ones of Shorer [35] and MCDF ones of Fielder, Lin, and Ton-That [39]. Small discrepancies of the $f_L$ values among the three method are observed in the table. The RCI results for the $2p_{3/2}\rightarrow 3s$ transitions are close to the MCDF

ones, whereas those for the $2p$-$3d$ transitions are close to the RRPA ones.

### B. $Ti^{12+}$ ion

In Table IV, the RCI transition energies for the same $E1$ transition in $Ti^{12+}$ are compared with experiment [36]. One sees from the table that the calculated energies are in good agreement with experiment except those for the $2p_{1/2} \rightarrow 5d_{3/2}$ transition. This is due to the limited basis set with $n \leq 5$ used in the present RCI calculation, since the mixing of wave functions between these states and higher excited states increases as their energy levels become closer to each other. Relatively large errors of the RCI results for these states due to the excitations of inner $2s$ and $2p_{1/2}$ electrons are also observed in the system.

The RCI $f_L$ values are compared with those with various theoretical calculations listed in the data table of Mori *et al.* [36]. The RCI oscillator strengths are in good agreement with those for most transitions except that for the $2p_{1/2} \rightarrow 5d_{3/2}$ transition which has just been discussed above. The oscillator strength for the resonance transition between the ground and the $2p_{1/2} \rightarrow 3d_{3/2}$ excited states becomes slightly large compared with that in $Ar^{8+}$ ion in Table III.

### C. $Fe^{16+}$ ion

In Table V, we compare the RCI transition energies for the $E1$ transitions in $Fe^{16+}$ with the experimental ones [34]. For the states up to $n=4$, experimental data are complete. It is seen from the table that the RCI excitation energies are in much better agreement with experiment than those for $Ar^{8+}$ and $Ti^{12+}$ ions. One also observes larger error for calculated results for the excitations of inner $2s$ and $2p_{1/2}$ electrons compared with those due to the excitation of the valence $2p_{3/2}$ electron. It is interesting to note that the absolute values of the error for all excited states up to $n=4$ are almost the same. It is considered that this arises mainly from the difference of the magnitude of the Lamb shift or the QED effects on the binding energy between the core electrons in the $L$ shell. As has been mentioned in Sec. III B, error in the RCI transition energies for some $n=2 \rightarrow 5$ transitions especially for the $2p_{1/2} \rightarrow 5d_{3/2}$ one becomes large compared with those for the $n=2 \rightarrow 3$ and the $n=2 \rightarrow 4$ transitions because the basis set used is not sufficient to de-

TABLE III. Transition energies and oscillator strengths with the length form $f_L$ for the $E1$ transitions from the ground state to the excited states with $J=1$ and odd parity in neonlike Ar($Z=18$).

| State | Transition energy ($cm^{-1}$) RCI | Expt.[a] | $\Delta E$ | $f_L$ RCI | RRPA[b] |
|---|---|---|---|---|---|
| $2s^22p^53s\ (\frac{3}{2},\frac{1}{2})^o_1$ | 2 044 048 | 2 033 350 | 10 698 | 0.0522 | 0.063 (0.050)[c] |
| $2s^22p^53s\ (\frac{1}{2},\frac{1}{2})^o_1$ | 2 063 460 | 2 052 120 | 11 340 | 0.1022 | 0.181 (0.112)[c] |
| $2s^22p^53d\ (\frac{3}{2},\frac{3}{2})^o_1$ | 2 361 937 | 2 349 620 | 12 317 | 0.0022 | 0.005 (0.001)[c] |
| $2s^22p^53d\ (\frac{1}{2},\frac{3}{2})^o_1$ | 2 392 145 | 2 379 820 | 12 325 | 0.1296 | 0.139 (0.175)[c] |
| $2s^22p^53d\ (\frac{1}{2},\frac{3}{2})^o_1$ | 2 431 187 | 2 410 800 | 20 387 | 2.1924 | 1.90 (1.85)[c] |
| $2s^22p^54s\ (\frac{3}{2},\frac{1}{2})^o_1$ | 2 718 302 | | | 0.0194 | |
| $2s^22p^54s\ (\frac{1}{2},\frac{1}{2})^o_1$ | 2 734 572 | | | 0.0054 | |
| $2s2p^63p\ (\frac{1}{2},\frac{1}{2})^o_1$ | 2 806 990 | 2 782 000 | 24 990 | 0.0027 | |
| $2s2p^63p\ (\frac{1}{2},\frac{3}{2})^o_1$ | 2 816 798 | 2 791 740 | 25 058 | 0.3252 | |
| $2s^22p^54d\ (\frac{3}{2},\frac{3}{2})^o_1$ | 2 834 792 | 2 834 470 | 322 | 0.0000 | |
| $2s^22p^54d\ (\frac{3}{2},\frac{5}{2})^o_1$ | 2 850 486 | 2 855 510 | −5 024 | 0.1145 | |
| $2s^22p^54d\ (\frac{1}{2},\frac{3}{2})^o_1$ | 2 868 985 | | | 0.5747 | |
| $2s^22p^55s\ (\frac{3}{2},\frac{1}{2})^o_1$ | 3 045 631 | | | 0.0174 | |
| $2s^22p^55d\ (\frac{3}{2},\frac{5}{2})^o_1$ | 3 056 381 | 3 063 730 | −7 349 | 0.1161 | |
| $2s^22p^55s\ (\frac{1}{2},\frac{1}{2})^o_1$ | 3 063 863 | | | 0.0536 | |
| $2s^22p^55d\ (\frac{3}{2},\frac{3}{2})^o_1$ | 3 230 103 | | | 0.1156 | |
| $2s^22p^55d\ (\frac{1}{2},\frac{3}{2})^o_1$ | 3 264 987 | | | 0.4808 | |
| $2s2p^64p\ (\frac{1}{2},\frac{1}{2})^o_1$ | 3 389 145 | | | 0.0018 | |
| $2s2p^64p\ (\frac{1}{2},\frac{3}{2})^o_1$ | 3 392 724 | | | 0.1038 | |
| $2s2p^65p\ (\frac{1}{2},\frac{3}{2})^o_1$ | 3 751 858 | | | 0.0740 | |
| $2s2p^65p\ (\frac{1}{2},\frac{1}{2})^o_1$ | 3 760 629 | | | 0.0946 | |

[a]Reference [34].
[b]Reference [35].
[c]Reference [39].

TABLE IV. Transition energies and oscillator strengths with the length form $f_L$ for the $E1$ transitions from the ground state in neonlike Ti($Z=22$).

| State | Transition energy ($cm^{-1}$) RCI | Expt.[a] | $\Delta E$ | $f_L$ RCI | Others[a] |
|---|---|---|---|---|---|
| $2s^22p^53s\ (\frac{3}{2},\frac{1}{2})^o_1$ | 3 720 398 | 3 709 200 | 11 198 | 0.0740 | 0.063 |
| $2s^22p^53s\ (\frac{1}{2},\frac{1}{2})^o_1$ | 3 764 133 | 3 753 600 | 10 533 | 0.0637 | 0.075 |
| $2s^22p^53d\ (\frac{3}{2},\frac{3}{2})^o_1$ | 4 179 077 | 4 168 200 | 10 877 | 0.0038 | |
| $2s^22p^53d\ (\frac{3}{2},\frac{5}{2})^o_1$ | 4 232 070 | 4 219 800 | 12 270 | 0.2948 | 0.33 |
| $2s^22p^53d\ (\frac{1}{2},\frac{3}{2})^o_1$ | 4 303 630 | 4 281 600 | 22 030 | 2.5675 | 2.4 |
| $2s2p^63p\ (\frac{1}{2},\frac{1}{2})^o_1$ | 4 759 835 | 4 733 300 | 26 535 | 0.0141 | |
| $2s2p^63p\ (\frac{1}{2},\frac{3}{2})^o_1$ | 4 781 061 | 4 754 000 | 27 061 | 0.2976 | |
| $2s^22p^54s\ (\frac{3}{2},\frac{1}{2})^o_1$ | 4 982 111 | 4 966 500 | 15 611 | 0.0114 | 0.017 |
| $2s^22p^54s\ (\frac{1}{2},\frac{1}{2})^o_1$ | 5 026 506 | 5 014 300 | 12 206 | 0.0084 | 0.011 |
| $2s^22p^54d\ (\frac{3}{2},\frac{3}{2})^o_1$ | 5 154 742 | | | 0.0045 | |
| $2s^22p^54d\ (\frac{3}{2},\frac{5}{2})^o_1$ | 5 179 380 | 5 163 700 | 15 680 | 0.3157 | 0.28 |
| $2s^22p^54d\ (\frac{1}{2},\frac{3}{2})^o_1$ | 5 223 496 | 5 207 200 | 16 296 | 0.4844 | 0.45 |
| $2s^22p^55s\ (\frac{3}{2},\frac{1}{2})^o_1$ | 5 528 602 | | | 0.0041 | |
| $2s^22p^55s\ (\frac{1}{2},\frac{1}{2})^o_1$ | 5 573 484 | | | 0.0033 | |
| $2s^22p^55d\ (\frac{3}{2},\frac{5}{2})^o_1$ | 5 608 281 | 5 596 300 | 11 981 | 0.1713 | 0.14 |
| $2s^22p^55d\ (\frac{3}{2},\frac{3}{2})^o_1$ | 5 689 532 | | | 0.0818 | |
| $2s^22p^55d\ (\frac{1}{2},\frac{3}{2})^o_1$ | 5 749 066 | 5 641 100 | 107 966 | 0.3044 | 0.16 |
| $2s2p^64p\ (\frac{1}{2},\frac{1}{2})^o_1$ | 5 894 831 | | | 0.0074 | |
| $2s2p^64p\ (\frac{1}{2},\frac{3}{2})^o_1$ | 5 901 081 | | | 0.1184 | |
| $2s2p^65p\ (\frac{1}{2},\frac{3}{2})^o_1$ | 6 483 758 | | | 0.0496 | |
| $2s2p^65p\ (\frac{1}{2},\frac{1}{2})^o_1$ | 6 491 695 | | | 0.0830 | |

[a]Reference [36].

TABLE V. Transition energies and oscillator strengths with the length form $f_L$ for the $E1$ transitions from the ground state in neonlike Fe($Z=26$).

| State | Transition energy ($cm^{-1}$) RCI | Expt.[a] | $\Delta E$ | $f_L$ RCI | Others[a] |
|---|---|---|---|---|---|
| $2s^22p^53s\ (\frac{3}{2},\frac{1}{2})^o_1$ | 5 875 609 | 5 864 770 | 10 839 | 0.0829 | 0.122 |
| $2s^22p^53s\ (\frac{1}{2},\frac{1}{2})^o_1$ | 5 969 957 | 5 960 870 | 9 087 | 0.0447 | 0.105 |
| $2s^22p^53d\ (\frac{3}{2},\frac{3}{2})^o_1$ | 6 482 760 | 6 471 800 | 10 960 | 0.0049 | 0.001 |
| $2s^22p^53d\ (\frac{3}{2},\frac{5}{2})^o_1$ | 6 564 236 | 6 552 200 | 12 036 | 0.6189 | 0.629 |
| $2s^22p^53d\ (\frac{1}{2},\frac{3}{2})^o_1$ | 6 680 481 | 6 660 000 | 20 481 | 2.5501 | 2.31 |
| $2s2p^63p\ (\frac{1}{2},\frac{1}{2})^o_1$ | 7 225 645 | 7 198 900 | 26 745 | 0.0305 | 0.029 |
| $2s2p^63p\ (\frac{1}{2},\frac{3}{2})^o_1$ | 7 260 860 | 7 234 300 | 26 560 | 0.3148 | 0.28 |
| $2s^22p^54s\ (\frac{3}{2},\frac{1}{2})^o_1$ | 7 900 034 | 7 885 800 | 14 234 | 0.0133 | 0.022 |
| $2s^22p^54s\ (\frac{1}{2},\frac{1}{2})^o_1$ | 7 997 853 | 7 983 000 | 14 853 | 0.0067 | 0.025 |
| $2s^22p^54d\ (\frac{3}{2},\frac{3}{2})^o_1$ | 8 132 412 | 8 116 000 | 16 412 | 0.0033 | 0.004 |
| $2s^22p^54d\ (\frac{3}{2},\frac{5}{2})^o_1$ | 8 168 769 | 8 154 000 | 14 769 | 0.4095 | 0.40 |
| $2s^22p^54d\ (\frac{1}{2},\frac{3}{2})^o_1$ | 8 260 958 | 8 249 000 | 11 958 | 0.4168 | 0.53 |
| $2s^22p^55s\ (\frac{3}{2},\frac{1}{2})^o_1$ | 8 773 600 | 8 757 000 | 16 600 | 0.0043 | 0.007 |
| $2s^22p^55s\ (\frac{1}{2},\frac{1}{2})^o_1$ | 8 872 484 | 8 860 000 | 12 484 | 0.0002 | 0.004 |
| $2s^22p^55d\ (\frac{3}{2},\frac{5}{2})^o_1$ | 8 899 330 | 8 887 000 | 12 330 | 0.2105 | 0.13 |
| $2s2p^64p\ (\frac{1}{2},\frac{1}{2})^o_1$ | 9 085 388 | 9 056 000 | 29 388 | 0.0183 | 0.016 |
| $2s2p^64p\ (\frac{1}{2},\frac{3}{2})^o_1$ | 9 097 026 | 9 072 000 | 25 026 | 0.1117 | 0.11 |
| $2s^22p^55d\ (\frac{3}{2},\frac{3}{2})^o_1$ | 9 689 956 | | | 0.1157 | |
| $2s^22p^55d\ (\frac{1}{2},\frac{3}{2})^o_1$ | 9 829 893 | 8 982 000 | 847 893 | 0.4604 | 0.18 |
| $2s2p^65p\ (\frac{1}{2},\frac{1}{2})^o_1$ | 9 925 981 | 9 878 000 | 47 981 | 0.0003 | |
| $2s2p^65p\ (\frac{1}{2},\frac{3}{2})^o_1$ | 9 929 645 | 9 878 000 | 51 645 | 0.0727 | |

[a]Reference [34].

scribe wave functions for these excited states adequately.

Concerning the oscillator strength for the $E1$ transitions considered in this ion, the RCI $f_L$ values for all the transitions except the $n=2\rightarrow5$ ones are consistent with those with other theoretical methods [34], where the $f_L$ values for the $2p\rightarrow3s$ and $2p\rightarrow3d$ transitions listed in the last column in the table are the RRPA ones of Shorer.

### D. $Ni^{18+}$ ion

In Table VI, the RCI and experimental transition energies [37] for the same transitions in $Ni^{18+}$ are compared. The experimental data for the transitions up to $n=4$ in this ion are also complete. Because of more increase of relativistic effects on binding energies for inner-shell electrons than outer-shell ones in heavier elements, the order of the excited states having electrons in the shells with $n=4$ and 5 are reversed in Fe and Ni ions. Good agreement between the theoretical and experimental transition frequencies are seen in the table except those for two excited states arising from the $2p_{3/2}\rightarrow5d_{5/2}$ and $2p_{1/2}\rightarrow5d_{3/2}$ transitions. The errors of the RCI energies for the states arising from the excitations of $2s$ to $4p_{1/2}$ and $4p_{3/2}$ states become small compared with those for the $2s\rightarrow4p$ transitions in $Fe^{16+}$ ion in Table V. One of the reasons for it may be due to strong mixing between these and $5d$ higher excited states in the RCI calculation because the level crossing between the $2p$-$5d$ and $2s$-$4p$ states happens in this ion. The level crossing for the excited states with $J=1$ and odd parity will be shown in the following section.

It is seen from the table that the calculated oscillator strengths between the RCI and other theoretical methods [37] for various transitions in the ion agree well, although some discrepancies of the $f_L$ values for several weak transitions between these two calculations are observed.

### E. $Mo^{32+}$ ion

In Table VII, we compare the RCI and experimental transition energies [40] for the $E1$ transitions in the $Mo^{32+}$ ion. Accuracy of the transition energies observed is not so good as those for other ions listed in Tables III–VI. It seems that the differences between the RCI and experimental transition energies for some transitions do not remain within a maximum allowed error which has been confirmed in other systems discussed above, where not only are the signs of the errors irregular but also their absolute values for some transitions are too large. However, one can observe good agreement between the RCI and the experimental transition energies for the resonance $2p\rightarrow3d$ transitions having large oscillator strengths.

Calculated $f_L$ values for the five $n=2\rightarrow3$ transitions by the RCI and RRPA methods are on the whole in agreement with each other. It is interesting to see that the values of the oscillator strength between the two $2p\rightarrow3s$ transitions and also between the two $2p\rightarrow3d$ ones are reversed in this ion, respectively. This is not the case for other ions with smaller $Z$ than the Mo ion.

TABLE VI. Transition energies and oscillator strengths with the length form $f_L$ for the $E1$ transitions from the ground state in neonlike Ni($Z=28$).

| State | Transition energy ($cm^{-1}$) | | | $f_L$ | |
|---|---|---|---|---|---|
| | RCI | Expt.[a] | $\Delta E$ | RCI | Others[a] |
| $2s^22p^53s\ (\frac{3}{2},\frac{1}{2})^o_1$ | 7 132 277 | 7 121 000 | 11 277 | 0.0861 | 0.125 |
| $2s^22p^53s\ (\frac{1}{2},\frac{1}{2})^o_1$ | 7 265 147 | 7 257 400 | 7 747 | 0.0386 | 0.098 |
| $2s^22p^53d\ (\frac{3}{2},\frac{3}{2})^o_1$ | 7 818 116 | 7 805 200 | 12 916 | 0.0053 | 0.009 |
| $2s^22p^53d\ (\frac{3}{2},\frac{5}{2})^o_1$ | 7 915 807 | 7 901 400 | 14 407 | 0.8201 | 0.80 |
| $2s^22p^53d\ (\frac{1}{2},\frac{3}{2})^o_1$ | 8 063 485 | 8 041 800 | 21 685 | 2.4635 | 2.2 |
| $2s2p^63p\ (\frac{1}{2},\frac{1}{2})^o_1$ | 8 652 757 | 8 621 400 | 31 357 | 0.0401 | 0.038 |
| $2s2p^63p\ (\frac{1}{2},\frac{3}{2})^o_1$ | 8 698 186 | 8 666 300 | 31 886 | 0.3210 | 0.29 |
| $2s^22p^54s\ (\frac{3}{2},\frac{1}{2})^o_1$ | 9 605 323 | 9 585 000 | 20 323 | 0.0142 | 0.023 |
| $2s^22p^54s\ (\frac{1}{2},\frac{1}{2})^o_1$ | 9 742 996 | 9 725 000 | 17 996 | 0.0057 | 0.024 |
| $2s^22p^54d\ (\frac{3}{2},\frac{3}{2})^o_1$ | 9 870 679 | 9 845 000 | 25 679 | 0.0041 | 0.003 |
| $2s^22p^54d\ (\frac{3}{2},\frac{5}{2})^o_1$ | 9 911 954 | 9 891 000 | 20 954 | 0.4456 | 0.43 |
| $2s^22p^54d\ (\frac{1}{2},\frac{3}{2})^o_1$ | 10 041 487 | 10 023 000 | 18 487 | 0.3780 | 0.49 |
| $2s^22p^55s\ (\frac{3}{2},\frac{1}{2})^o_1$ | 10 676 730 | | | 0.0048 | |
| $2s^22p^55s\ (\frac{1}{2},\frac{1}{2})^o_1$ | 10 814 261 | | | 0.0466 | |
| $2s^22p^55d\ (\frac{3}{2},\frac{5}{2})^o_1$ | 10 821 863 | 10 797 000 | 24 863 | 0.1156 | |
| $2s^22p^55d\ (\frac{3}{2},\frac{3}{2})^o_1$ | 10 871 744 | 10 806 000 | 65 744 | 0.0884 | 0.12 |
| $2s2p^64p\ (\frac{1}{2},\frac{1}{2})^o_1$ | 10 942 650 | 10 925 000 | 17 650 | 0.0138 | 0.020 |
| $2s2p^64p\ (\frac{1}{2},\frac{3}{2})^o_1$ | 10 958 022 | 10 941 000 | 17 022 | 0.1027 | 0.12 |
| $2s^22p^55d\ (\frac{1}{2},\frac{3}{2})^o_1$ | 11 025 999 | 10 942 000 | 83 999 | 0.2183 | 0.18 |
| $2s2p^65p\ (\frac{1}{2},\frac{1}{2})^o_1$ | 11 980 054 | | | 0.0109 | |
| $2s2p^65p\ (\frac{1}{2},\frac{3}{2})^o_1$ | 11 987 818 | | | 0.0734 | |

[a]Reference [37].

### F. Z-dependent behavior of the transition frequencies and oscillator strengths in neonlike systems

It is interesting to examine the $Z$ dependence of the transition frequency and the oscillator strength in an isoelectronic sequence because the variation of the various relativistic and QED effects on the energies and wave functions in each system leads to a systematic change of the transition energy and the oscillator strength in isoelectronic atomic systems [41].

In Fig. 4, the variation of the order of excited levels for odd-parity states with $J=1$ in neon isoelectronic sequence considered here is shown schematically to see where level crossings occur in the isoelectronic sequence. In the figure, each excited state is designated by a main configuration obtained for $Ar^{8+}$ as the $LS$ coupling region and for $U^{92+}$ as the $j$-$j$ coupling region in the left and right sides, respectively. Main CSF's in $j$-$j$ coupling obtained for corresponding excited states are not always outstanding in the $LS$ coupling region, whereas each excited state in neonlike systems with $Z>40$ can be well be designated by a main CSF in $j$-$j$ coupling obtained with RCI calculation. For the excited states expressed by the single-excitation CSF's of the $n=2\rightarrow3$ and $n=2\rightarrow4$ transitions, $ns^{L,U}$, $nd^{L,M,U}$, and $np^{L,U}$ states in the $LS$ coupling region correspond to $2p_{1/2,3/2}\rightarrow ns$, $2p_{3/2}\rightarrow nd_{3/2,5/2}$ and $2p_{1/2}\rightarrow nd_{3/2}$, and $2s\rightarrow np_{1/2,3/2}$ states in the $j$-$j$ coupling region, respectively. However, for the $n=5$ excited states, this correspondence between the two coupling regions does not hold for the $5d^L$, $5d^M$, $5p^L$, and $5p^U$ states, where the level crossings between the $5d^L$ and $5d^M$ and between the $5p^L$ and $5p^U$ states occur as the atomic number increases. As the basis set used is not enough to obtain accurate excitation energies for the $n=5$ excited states, we do not discuss the energies for the $n=2\rightarrow5$ excited states further.

It is seen from Fig. 4 that many level crossings appear when $Z$ becomes large. The level crossing depending on $Z$ shows that the magnitude of the relativistic effects on the binding energy for each electron increases in a different way when the atomic number increases. In a system at a crossing point in the figure, the wave functions between the two states mix largely. This leads to a sudden change in the oscillator strength for a transition in a certain specific position of an isoelectronic sequence. This type of anomaly in the oscillator strength has been explained as the CI effects for the wave functions as a result of drawing the two levels in a system of an isoelectronic sequence [42]. Such an anomaly in the oscillator strength for the $E1$ transitions of $n=2\rightarrow3$ and $n=2\rightarrow4$ in neon isoelectronic sequence will be shown in the following part of this section.

Shorer [35] has shown the $Z$-dependent behavior of the oscillator strength for the five $E1$ transitions of $n=2\rightarrow3$, that is, two $2p\rightarrow3s$ and three $2p\rightarrow3d$ ones, in neon isoelectronic sequence with the RRPA calculation, where some anomalies in the oscillator strength for the $E1$ transitions in this sequence have been shown. We have

TABLE VII. Transition energies and oscillator strengths with the length form $f_L$ for the $E1$ transitions from the ground state in neonlike Mo($Z=42$).

| State | Transition energy ($cm^{-1}$) RCI | Expt.[a] | $\Delta E$ | $f_L$ RCI | RRPA[b] |
|---|---|---|---|---|---|
| $2s^22p^53s\ (\frac{3}{2},\frac{1}{2})^o_1$ | 19 211 890 | 19 220 000 | −8 110 | 0.0960 | 0.132 |
| $2s^22p^53s\ (\frac{1}{2},\frac{1}{2})^o_1$ | 20 063 934 | 20 080 000 | −16 066 | 0.0171 | 0.084 |
| $2s^22p^53d\ (\frac{3}{2},\frac{3}{2})^o_1$ | 20 590 301 | 20 612 000 | −21 699 | 0.0005 | 0.001 |
| $2s^22p^53d\ (\frac{3}{2},\frac{5}{2})^o_1$ | 20 825 558 | 20 814 000 | 11 558 | 1.9454 | 1.82 |
| $2s^22p^53d\ (\frac{1}{2},\frac{3}{2})^o_1$ | 21 600 506 | 21 593 000 | 7 506 | 1.6837 | 1.62 |
| $2s2p^63p\ (\frac{1}{2},\frac{1}{2})^o_1$ | 22 434 767 | 22 398 000 | 36 767 | 0.0976 | |
| $2s2p^63p\ (\frac{1}{2},\frac{3}{2})^o_1$ | 22 674 560 | 22 634 000 | 40 560 | 0.3473 | |
| $2s^22p^54s\ (\frac{3}{2},\frac{1}{2})^o_1$ | 26 120 752 | 26 250 000 | −129 248 | 0.0174 | |
| $2s^22p^54d\ (\frac{3}{2},\frac{3}{2})^o_1$ | 26 664 600 | | | 0.0002 | |
| $2s^22p^54d\ (\frac{3}{2},\frac{5}{2})^o_1$ | 26 752 892 | 27 140 000 | −387 108 | 0.5110 | |
| $2s^22p^54s\ (\frac{1}{2},\frac{1}{2})^o_1$ | 26 988 471 | 26 570 000 | 418 471 | 0.0158 | |
| $2s^22p^54d\ (\frac{1}{2},\frac{3}{2})^o_1$ | 27 581 464 | 27 500 000 | 81 464 | 0.2826 | |
| $2s2p^64p\ (\frac{1}{2},\frac{1}{2})^o_1$ | 29 016 609 | | | 0.0439 | |
| $2s2p^64p\ (\frac{1}{2},\frac{3}{2})^o_1$ | 29 114 983 | | | 0.1108 | |
| $2s^22p^55s\ (\frac{3}{2},\frac{1}{2})^o_1$ | 29 223 160 | | | 0.0032 | |
| $2s^22p^55d\ (\frac{3}{2},\frac{3}{2})^o_1$ | 29 455 799 | | | 0.0009 | |
| $2s^22p^55d\ (\frac{3}{2},\frac{5}{2})^o_1$ | 29 494 374 | 29 200 000 | 294 374 | 0.2144 | |
| $2s^22p^55s\ (\frac{1}{2},\frac{1}{2})^o_1$ | 30 093 277 | | | 0.0052 | |
| $2s^22p^55d\ (\frac{1}{2},\frac{3}{2})^o_1$ | 30 348 908 | 30 100 000 | 248 908 | 0.1073 | |
| $2s2p^65p\ (\frac{1}{2},\frac{1}{2})^o_1$ | 31 976 186 | | | 0.0166 | |
| $2s2p^65p\ (\frac{1}{2},\frac{3}{2})^o_1$ | 32 025 472 | | | 0.0394 | |

[a]Reference [40].
[b]Reference [35].

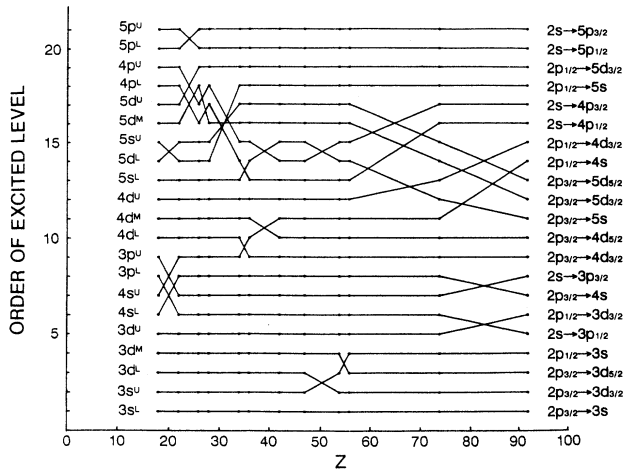


FIG. 4. Order of the excited levels with $J=1$ and odd parity from lower to higher states in neon isoelectronic sequence. $ns^{L,U}$, $nd^{L,M,U}$, and $np^{L,U}$ in the $LS$ coupling region stand for the lower and upper $2p\rightarrow ns$, the lower, middle, and upper $2p\rightarrow nd$, and the lower and upper $2s\rightarrow np$ excited states for $n=3\rightarrow 5$, respectively. In the $j$-$j$ coupling region, main configurations for the states are given by the single-excitation states as $2p_{3/2}\rightarrow ns$, $2p_{1/2}\rightarrow ns$, $2p_{3/2}\rightarrow nd_{3/2}$, $2p_{3/2}\rightarrow nd_{5/2}$, $2p_{1/2}\rightarrow nd_{3/2}$, $2s\rightarrow np_{1/2}$, and $2s\rightarrow np_{1/2}$ for $n=3\rightarrow 5$.

shown in the preceding section that our $f_L$ values for the same $n=2\rightarrow 3$ transitions in some neonlike systems agree well with those of Shorer.

In Fig. 5, the RCI $f_L$ values for the seven $E1$ transitions of $n=2\rightarrow 3$ in 12 neonlike systems between $Ar^{8+}$ and $U^{82+}$ are shown as a function of $Z$. The magnitude of the $f$ value for the $2p_{1/2}\rightarrow 3d_{3/2}$ transition, which is the largest for the systems with around $Z<40$, has a maximum at $Z=22$ and decreases monotonously as the atomic number $Z$ increases. On the other hand, the $f$ value for the $2p_{3/2}\rightarrow 3d_{5/2}$ transition grows drastically as a function of $Z$ up to 47 and decreases slightly at around $Z=56$. However, it keeps the largest value for all the $E1$ transitions in systems with $Z>40$. It is also seen in the figure that the oscillator strengths for the rest $n=2\rightarrow 3$ transitions are small compared with those for the two $2p\rightarrow 3d$ resonance transitions described above and change little all over $Z$ except that for the $2p_{1/2}\rightarrow 3s$ transition which suddenly increases for $Xe^{44+}$ and $Ba^{46+}$ in the isoelectronic sequence. This anomaly in the oscillator strength for the $2p_{1/2}\rightarrow 3s$ transition is closely connected with the decrease of those for the two $2p$-$3d$ resonance. The reason for this can be clarified by finding the level crossing in the isoelectronic sequence. In Fig. 4, one sees that the energy level for the $3s^U$ state, which corresponds to the $2p_{1/2}\rightarrow 3s$ transition state, crosses the levels for the two excited levels corresponding to the $2p_{3/2}\rightarrow 3d_{5/2}$ and $2p_{1/2}\rightarrow 3d_{3/2}$ transition states in $Xe^{44+}$ and $Ba^{46+}$, respectively. In these systems, the mixing of the wave functions for these excited states becomes large so that the redistribution of the oscillator strength among these $E1$ transitions occurs.

For the $n=2\rightarrow 4$ transitions in the same neonlike systems, the RCI $f_L$ values are plotted as a function of $Z$ in Fig. 6. The $f$ values for the $n=2\rightarrow 4$ transitions are about a quarter as small as those for the corresponding $n=2\rightarrow 3$ transitions in the isoelectronic sequence shown in Fig. 5. However, it seems that the $Z$-dependent behavior for the oscillator strength between the $n=2\rightarrow 3$ and $n=2\rightarrow 4$ transitions in this sequence is similar, although the curves of the $f$ value as a function of $Z$ for all the $n=2\rightarrow 4$ transitions are slightly shifted to the lower $Z$ direction compared with those for the $n=2\rightarrow 3$ transitions. So it is seen in the figure that there is no maximum of the $f$ value for the $2p_{1/2}\rightarrow 4d_{3/2}$ resonance transition in elements heavier than Ar. On the other hand, the oscillator strength for this resonance transition in neon isoelectronic sequence decreases significantly in $W^{64+}$ and recovers a normal value in $U^{82+}$. This anomaly in the $f$ value can also be explained as the CI effects between this state and the $n=5$ excited one under consideration, since it is seen in Fig. 4 that the excited level

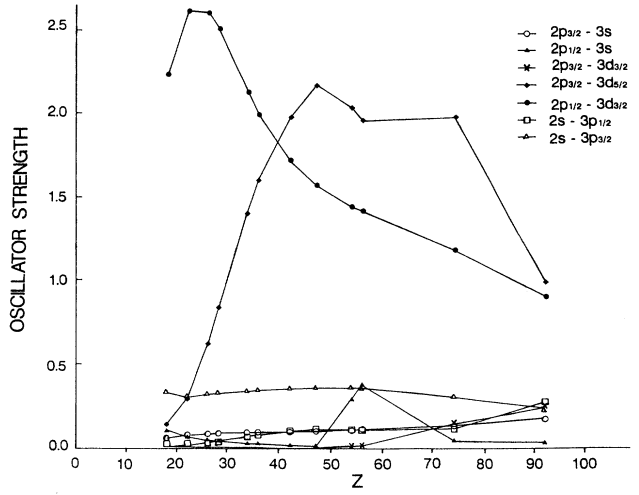


FIG. 5. Variation of the oscillator strength for the $n=2\rightarrow 3$ transitions in neon isoelectronic sequence.

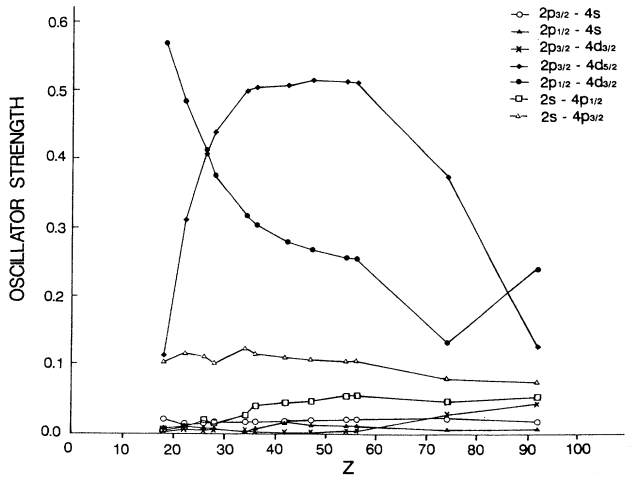


FIG. 6. Variation of the oscillator strength for the $n=2\rightarrow 4$ transitions in neon isoelectronic sequence.

corresponding to the $2p_{1/2} \rightarrow 4d_{3/2}$ transition goes up gradually as the $Z$ increases and crosses some $n=5$ excited levels at around $Z=70$ near tungsten. The CI effects for the oscillator strength also cause the change of $f$ values for the $n=2 \rightarrow 5$ transitions, which is not shown here. One also sees in Fig. 5 that the oscillator strength for the $2p_{1/2} \rightarrow 4s$ transition has two small peaks at $Z=22$ and 42. These changes of the oscillator strength are expected since the $4s^U$ level which corresponds to the $2p_{1/2} \rightarrow 4s$ excited state crosses the $3p^U$ state near $Z=22$ and the $4d^M$ level near $Z=42$ in Fig. 4. In fact it is found in Figs. 5 and 6 that the oscillator strengths for the $2s \rightarrow 3p_{1/2}$ transition in $Ti^{12+}$ and for the $2p_{3/2} \rightarrow 4d_{5/2}$ one in $Mo^{32+}$ are diminished slightly in neon isoelectronic sequence.

## IV. SUMMARY AND CONCLUSIONS

We have presented the relativistic configuration-interaction theory for atomic systems with an analytical relativistic Hartree-Fock-Roothaan function as a basis set. The basis set for constructing CSF's consists of all real and virtual RHFR one-electron functions expanded in terms of Slater-type orbitals. The total wave function is written as a linear combination of CSF's. The Breit interaction operator is treated by the first-order-perturbation theory.

In order to see the effectiveness of the method, numerical application of it to various neonlike atomic systems has been carried out. It has been shown that the RCI method yields good excitation energies in the systems by comparing the calculated results with experiment. Small discrepancy between the calculated excitation energies and experimental ones is due not only to the limited basis set used but also to the lack of the Lamb shift or the QED corrections in the RCI theory. The present RCI method has the merit that one can save much computation time when obtaining a large number of multiplet states in atomic systems because of an analytical form of the basis set. The theoretical transition energies and oscillator strengths for various transitions obtained for an atomic isoelectronic sequence will be very useful in identifying the lines observed.

As has been mentioned above, comparison of the RCI excitation energies with experiment in various neonlike systems shows the importance of the Lamb shift or the QED effects in obtaining a good energy with high accuracy. However, the method of calculating such higher-order correction energies for many-electron systems has not been established yet. Another important effect on the total energy in many-electron systems is the electron correlation effect. In the relativistic case, it is impossible to treat the two effects separately in the theory because they are coupled in various ways through the interaction between electrons.

In the RCI method, the calculated results for a system deeply depend on the basis set used especially for higher excited states. This means that it is important to examine the completeness of the basis set used in the RCI calculations. In order to obtain an accurate electron correlation energy for a system in the calculation, more one-electron functions must be included in the basis set. After the electron correlation effects on the energy in an atomic system are sufficiently taken into account in the calculation, an accurate QED correction energy in it could be estimated by subtracting the calculated energy from the experimental one.

## ACKNOWLEDGMENTS

We thank the Information Processing Center of Nara Women's University for the use of the FACOM M760/6 computer. This work was supported in part by a Grant-in-Aid from the Japanese Ministry of Education (Grant No. 02640293).

[1] B. C. Stratton, H. W. Moos, S. Suckewer, U. Feldman, J. F. Seely, and A. K. Bhatia, Phys. Rev. A **31**, 2534 (1985).
[2] Review articles in *Physics of Highly-Ionized Atoms,* Vol. 201 of *NATO Advanced Study Institute, Series B: Physics,* edited by R. Marrus (Plenum, New York, 1989).
[3] G. E. Brown and D. G. Ravenhall, Proc. R. Soc. London, Ser. A **208**, 552 (1951).
[4] M. Mitteleman, Phys. Rev. A **5**, 2395 (1972); **24**, 1167 (1981).
[5] J. Sucher, Phys. Rev. A **22**, 348 (1980).
[6] T. Kagawa and S. Kiyokawa, in *Abstracts of Contributed Papers of 12th ICAP,* edited by W. E. Baylis *et al.* (University of Michigan, Ann Arbor, 1990), pp. VII–40.
[7] I. P. Grant, Adv. Phys. **19**, 747 (1970).
[8] Y.-K. Kim, Phys. Rev. **154**, 17 (1967).
[9] T. Kagawa, Phys. Rev. A **12**, 2245 (1975).
[10] J. P. Desclaux, Comput. Phys. Commun. **9**, 31 (1975).
[11] I. P. Grant, B. J. McKenzie, P. H. Norrington, D. F. Mayers, and N. C. Pyper, Comput. Phys. Commun. **21**, 207 (1980).
[12] T. Kagawa, Phys. Rev. A **22**, 2340 (1980).
[13] M. Vajed-Samii, S. N. Ray, T. P. Das, and J. Andriessen, Phys. Rev. A **20**, 1787 (1979).
[14] W. R. Johnson and J. Sapirstein, Phys. Rev. Lett. **57**, 1126 (1986); S. A. Blundlell, W. R. Johnson, and J. Sapirstein, Phys. Rev. A **38**, 4961 (1988).
[15] Y. Ishikawa, Phys. Rev. A **42**, 1142 (1990).
[16] H. M. Quiney, I. P. Grant, and S. Wilson, J. Phys. B **23**, L271 (1990).
[17] U. I. Safronova and Z. B. Rudzikas, J. Phys. B **9**, 1989 (1976).
[18] P. L. Hagelstein, Phys. Rev. A **34**, 924 (1986).
[19] S. P. Goldman, Phys. Rev. A **36**, 3054 (1987).
[20] R. D. Cowan and D. C. Griffin, J. Opt. Soc. Am. **65**, 1989 (1976).
[21] G. Racah, Phys. Rev. **62**, 438 (1942); **63**, 367 (1943).
[22] U. Fano, Phys. Rev. **139**, A1042 (1965).
[23] U. Fano and G. Racah, *Irreducible Tensorial Sets* (Academic, New York, 1963).
[24] A. de-Shalit and I. Talmi, *Nuclear Shell Theory* (Academic, New York, 1959).
[25] R. D. Lawson and M. H. Macfarlane, Nucl. Phys. **66**, 80

(1965).
[26] L. Armstrong, Jr., Phys. Rev. **172**, 12 (1968); **172**, 18 (1968).
[27] B. R. Judd, *Second Quantization and Atomic Spectroscopy* (Johns Hopkins Press, Baltimore, 1967).
[28] F. Sasaki, Int. J. Quantum Chem. **8**, 605 (1974).
[29] I. P. Grant and N. C. Pyper, J. Phys. B **9**, 761 (1976).
[30] I. P. Grant, J. Phys. B **7**, 1458 (1974).
[31] L. Armstrong, Jr., W. R. Fielder, and D. L. Lin, Phys. Rev. A **14**, 1114 (1976).
[32] P. L. Hagelstein and R. K. Jung, At. Data Nucl. Data Tables **37**, 121 (1987).
[33] E. Biemont and J. E. Hansen, At. Data Nucl. Data Tables **37**, 1 (1987).
[34] T. Shirai, Y. Funakata, K. Mori, J. Sugar, W. L. Wiese, and Y. Nakai, J. Phys. Chem. Ref. Data **19**, 127 (1990).
[35] P. Shorer, Phys. Rev. A **20**, 642 (1979).
[36] K. Mori, W. L. Wiese, T. Shirai, Y. Nakai, K. Ozawa, and T. Kato, At. Data Nucl. Data Tables **34**, 79 (1986).
[37] T. Shirai, K. Mori, J. Sugar, W. L. Wiese, Y. Nakai, and K. Ozawa, At. Data Nucl. Data Tables **37**, 235 (1987).
[38] S. Bashkin and J. O. Stoner, Jr., *Atomic Energy Levels and Grotrian Diagrams* (North-Holland, Amsterdam, 1975), Vol. I.
[39] W. Fielder, Jr., Dong L. Lin, and Dinh Ton-That, Phys. Rev. A **19**, 741 (1979).
[40] T. Shirai, Y. Nakai, K. Ozawa, K. Ishii, J. Sugar, and K. Mori, J. Phys. Chem. Ref. Data **16**, 327 (1987).
[41] Y.-K. Kim and J. P. Desclaux, Phys. Rev. Lett. **36**, 139 (1976).
[42] A. W. Weiss, in *Beam Foil Spectroscopy,* edited by I. A. Sellin *et al.* (Plenum, New York, 1976), Vol. 1, pp. 51–68.